

Morphotectonic signatures and revised timing of opening of the Andaman Backarc Basin, Northeast Indian Ocean

**V. Yatheesh^{a,*}, K.K. Aswini^{a,b}, K.A. Kamesh Raju^{a,c}, J. John Savio^a,
Amol Gawas^a, Pawan Dewangan^a**

^aCSIR - National Institute of Oceanography, Dona Paula, Goa 403 004, India

^bSchool of Earth, Ocean and Atmospheric Sciences, Goa University,
Taleigao Plateau, Goa 403 206, India

^cNational Centre for Polar and Ocean Research, Ministry of Earth Sciences,
Vasco da Gama, Goa 403 804, India

* Corresponding author: E-mail address: yatheesh@nio.org; yatheeshv@gmail.com (V. Yatheesh)
Tel: +91 832 2450563; Fax: +91 832 2450602

Abstract

The Andaman Backarc Basin is believed to have been formed by the present episode of seafloor spreading in the Andaman Sea, separating the Alcock Rise in the north (Burmese Plate) and the Sewell Rise in the south (Sunda Plate). The geophysical investigations carried out so far in this basin provided detailed information on the morphotectonic signatures of its central sector, however, such understanding of the eastern sector is still awaited. Those studies also inferred continual seafloor spreading in the Andaman Backarc Basin starting from 4.0 Ma, however, some of the subsequent studies, based on deep water sedimentation, postulated an episodic seafloor spreading responsible for the formation of the Andaman Backarc Basin. To address these problems, we revisited the morphotectonic signatures and evolution of the Andaman Backarc Basin using a new set of multibeam bathymetry and magnetic data from the central and eastern sectors of the Andaman Backarc Basin, complemented by the existing geophysical data from the central sector. Our updated bathymetry map of the newly surveyed northernmost segment (referred as Segment D), is characterized by the presence of a well-defined rift valley, with an along-axis gentle dip from the west to the east. The segment D is also characterized by the absence of significant magnetic anomalies, as in the case of segment C, corroborating the concept of replacement of layer 2A by a sill-sediment-metasedimentary layer, in a sedimented spreading centre. Further, our revisit to the magnetic anomaly identifications suggests that the magnetic anomalies over the segment B of the Andaman Backarc Basin can reasonably be explained in terms of continual seafloor spreading from chron C3An.1ny (5.894 Ma) till the present (0.0 Ma). Based on these identifications of magnetic anomalies and the plate tectonic reconstructions, we revise the age of opening of the Andaman Backarc Basin from 4.0 Ma to ~5.9 Ma.

Key words: Andaman Backarc Basin; seafloor spreading; morphology; magnetic anomalies; isochrons

1. Introduction

The Andaman-Nicobar-Sumatra Subduction Zone is a convergent margin, where the Indian/Australian Plate is obliquely subducting beneath the Burmese/Sunda Plate, resulting in the formation of the Andaman Sea, which is bounded by the Andaman-Nicobar-Sumatra Trench in the west, Malay Peninsula in the east, Myanmar in the north and Sumatra in the South (Figure 1). The major tectonic domains that constitute the Andaman Sea are the Andaman-Nicobar-Sumatra Subduction Zone, fore arc basin, Alcock-Sewell rises and backarc basin. Although the nomenclatures used for most of these tectonic domains are consistent, several researchers used different nomenclatures for the backarc basin such as the Central Andaman Trough (Rodolfo, 1969), Andaman Sea Basin (Curry et al., 1979), Andaman Basin (Kamesh Raju et al., 2004), Central Andaman Basin (Curry, 2005), Andaman Backarc Spreading Centre (Kamesh Raju et al., 2004; Diehl et al., 2013), Andaman Sea Spreading Centre (Jourdain et al., 2016; Singh and Moeremans, 2017), etc., to represent the same tectonic domain. The intermittent usage of these nomenclatures creates confusion to the readers and therefore for the ease of reference, in this paper, we refer the ocean basin created by the present episode of seafloor spreading in the Andaman Sea as the Andaman Backarc Basin (ABB).

The bathymetry map (Figure 1a) of the Andaman Backarc Basin generated using the latest available GEBCO gridded bathymetry data (GEBCO Compilation Group, 2020) clearly depicts the existence of complex morphological features representing the deep ocean basins, linear ridge-like features and the anomalous bathymetric high complexes within this tectonic domain. From this bathymetry map, nearly E-W trending rift-valley-like features are clearly visible in the axial part of the deep ocean basin existing between the Alcock and Sewell rises, as well as in the region located northeast of the Alcock Rise. The morphotectonics of the central part of the Andaman Backarc Basin were thoroughly investigated by Kamesh Raju et al. (2004), and suggested that the spreading centre can be sub-divided into three segments, A, B, and C (Figure 2), all of which are associated with well-defined rift valleys. The bathymetry map (Figure 1a) suggests the possible presence of another spreading segment located northeast of the Alcock Rise, connected by an ~180 km long transform fault from the segment C (Figure 2). Detailed multibeam bathymetric investigation over this region to understand the morphotectonics of this possible spreading segment is still awaited.

The Andaman Backarc Basin is believed to have formed by the present episode of seafloor spreading in the backarc basin, separating the Alcock and Sewell rises. Among the three spreading centre segments (A, B and C) mapped in the Andaman Backarc Basin, only segment B is associated with identifiable seafloor spreading type magnetic anomalies. Based on the analysis of magnetic data along segment B, the seafloor spreading in the Andaman Backarc Basin was considered to have

initiated at around 11.0 Ma (Curry et al., 1979), but later, Kamesh Raju et al. (2004) revised this timing to 4.0 Ma. However, some of the recent studies (Morley, 2015; Morley and Alvey, 2015) reported that the sedimentary geometries are incompatible with continual seafloor spreading starting from 4.0 Ma till present, rather, this region is suggested to be associated with episodic seafloor spreading mostly from the middle to late Miocene, followed by a recent re-activation. Such an inference necessitates a revisit to the magnetic anomaly identifications over the segment B to evaluate the postulated incompatibility in the continual seafloor spreading.

In this study, we revisit the Andaman Backarc Basin with an aim to understand the morphotectonics of a possible fourth spreading segment located east of the Alcock Rise and to evaluate the postulated incompatibility in the continual seafloor spreading by reinterpreting the magnetic anomaly identifications, using a new set of multibeam bathymetry and additional magnetic data, complemented by those published by Kamesh Raju et al. (2004). The derived inferences are further used to generate plate tectonic reconstruction maps to depict the plate tectonic evolution of the Andaman Backarc Basin, starting from breakup of Alcock-Sewell Rise Complex till the present.

2. Tectonic framework

The Andaman-Nicobar-Sumatra Subduction Zone (Figure 2) is a typical accretionary-type subduction zone, associated with a well-defined trench, accretionary prism, forearc high, forearc basin, volcanic arc and backarc basin (Roy and Sharma, 1993). The trench along its entire extent is clearly identifiable from the satellite-derived free-air gravity anomaly map (Figure 1b), but in the bathymetry map (Figure 1a), the trench is visible south of 10°N only, since it is covered with Bengal Fan sediments in the north. The Ninetyeast Ridge located within the Indian/Australian plate subducts obliquely under the Andaman-Nicobar segment of the Andaman-Nicobar-Sumatra Trench, north of 8°N.

The accretionary prism, together with the forearc high, in the northern sector of the Andaman-Nicobar-Sumatra Subduction Zone is defined by the Andaman-Nicobar Ridge, over which the Andaman and Nicobar Islands are situated (Figure 2). The eastern boundary of the Andaman-Nicobar Ridge is defined by the Eastern Margin Fault (EMF) north of 8°30'N, and by the southern segment of the Andaman-Nicobar Fault (ANF) between 8°30'N and 7°N (Cochran, 2010; Singh et al., 2013). The region existing between the Eastern Margin Fault in the west and the Andaman-Nicobar Fault in the east represents the Andaman-Nicobar Forearc Basin. This forearc basin, located north of 8°30'N, is characterized by the presence of a prominent N-S trending fault, known as Diligent Fault (DLF), and a shallower N-S aligned ridge, referred to as the Invisible Bank (Singh et al., 2013; Singh and Moeremans, 2017). Some researchers (Curry, 2005) considered that the Invisible Bank (IB) is

underlain by uplifted volcanics and/or intrusives, while others (Singh and Moeremans, 2017) considered this feature as a continental fragment, which got rifted from Malay Peninsula during the early spreading stages in the Andaman Sea. Between 8°30'N and 7°N, forearc basin is absent and further southward exists the Aceh Forearc Basin, bordered by the West Andaman Fault (WAF) in the west and the Sumatra Island in the east (Mukti, 2018). The Great Sumatra Fault (GSF) defines the boundary between the Sunda Plate and the sliver plate in Sumatra. North of 5°N, the Great Sumatra Fault is bifurcated as the Aceh Fault (ACF) in the west and Seulimeum Fault (SLF) in the east. The southern portion of the Andaman-Nicobar Fault (from the southwest end of the Andaman Backarc Basin spreading centre till its point of intersection with the West Andaman Fault and the Aceh Fault) and the Seulimeum Fault together represents the boundary between the Sunda Plate and the Burmese Plate (Cochran, 2010; Singh et al., 2013).

The region located east of the Andaman-Nicobar Fault represents the Andaman Backarc Basin, which is considered to have been formed by seafloor spreading separating the Alcock and Sewell rises. The westernmost part of the Andaman Backarc Basin is characterized by the presence of several volcanoes that are part of the volcanic arc, east of Great Sumatran Fault and south of 6°N latitude. Between 6°26'N and 10°58'N, the region is characterized by the presence of 32 seamounts together forming a part of the active submarine volcanic arc (Kamesh Raju et al., 2004; Ghosal et al., 2012; Kamesh Raju et al., 2012; Tripathi et al., 2017; Aswini et al., 2020; Kamesh Raju et al., 2020). Among these, four seamounts are associated with well-developed craters (Kamesh Raju et al., 2012; Tripathi et al., 2017). The only volcanoes found further north are the currently active Barren Island volcano (Sheth et al., 2009) and the dormant Narcondam Island volcano (Bandopadhyay, 2017). The Alcock and Sewell rises are the two prominent bathymetric high complexes present within the Andaman Backarc Basin, named after Alfred William Alcock [1853-1933] and R.B. Seymour Sewell [1880-1964], respectively, considering their pioneering scientific investigations in the Andaman Sea (Rodolfo, 1969). The crustal thickness of the Alcock and Sewell rises derived based on the forward modelling of gravity anomalies are 15-20 km and 13 km, respectively, however, nature of the crust underlying these anomalous features are still debated. Some authors (Curry et al., 1979; Curry, 2005) considered oceanic crust origin based on the dating of available sparse rock samples, while others (Morley, 2015; Morley and Alvey, 2015) considered these features to represent hyper-thinned continental crust based on the gravity inversion. The region existing between the Alcock and Sewell rises is the Andaman Backarc Basin, which is considered to have formed by the present episode of seafloor spreading in the Andaman Sea. In majority of the subduction zones, the spreading segments in the backarc basins trend parallel (and spreading direction normal) to the trenches; however, the trend

of the spreading segments of present episode of seafloor spreading in the Andaman Backarc Basin is oblique (and spreading direction nearly parallel) to the Andaman-Nicobar-Sumatra Trench (Kamesh Raju et al., 2004). This seafloor spreading system consists of four spreading centre segments, offset by transform faults, connecting the Andaman-Nicobar Fault in the south and the Sagaing Fault (SGF) in the north (Curray et al., 1979; Kamesh Raju et al., 2004; Curray, 2005; Jourdain et al., 2016). The formation of the Andaman Backarc Basin was originally inferred to have initiated at 11.0 Ma (Curray et al., 1979), but later, Kamesh Raju et al. (2004) assigned an age of 4.0 Ma, based on the interpretation of closely-spaced marine magnetic profiles acquired in the Andaman Backarc Basin.

The deep ocean basin existing between the Sewell Rise and Mergui Ridge is known as the East Andaman Basin, which is underlain by thinned / stretched continental crust consisting of a series of tilted fault blocks and grabens (Jha et al., 2008). This region is inferred to represent a failed rift formed as a result of crustal divergence between Alcock-Sewell Rise Complex and the Mergui Ridge (Curray et al., 1979; Curray, 2005). The Mergui Basin, bounded in the west by the Mergui Ridge and in the east by Mergui Shelf, is considered to have formed during the oldest episode of crustal extension by rifting and thinning of the continental crust in the Oligocene (Curray et al., 1979; Curray, 2005). Based on the locations and strike of the graben and half-graben extensional faulting identified, the Mergui Basin is inferred to represent region of crustal extension, early E-W to WNW-ESE extension (Oligocene-Early Miocene) and later (Early Miocene to early Middle Miocene) NNW-SSE extension (Curray et al., 1979; Polachan and Racey, 1994; Curray, 2005; Srisuriyon and Morley, 2014; Morley, 2017; Morley and Searle, 2017).

3. Data and Methodology

The main data used in the present study are high-resolution multibeam bathymetry data as well as sea-surface magnetic profiles, acquired during SSD-046 expedition onboard *RV Sindhu Sadhana* by CSIR-National Institute of Oceanography (CSIR-NIO), Goa, India, during February-March, 2018. Multibeam bathymetry data were collected using Teledyne-Atlas multibeam echo sounders, operated at a frequency of 15 kHz. The magnetic data were collected using Geometrics 882 magnetometer. The magnetic measurements were reduced to magnetic anomalies, by applying the International Geomagnetic Reference Field (IGRF) of appropriate epoch. This underway geophysical database is complemented with those acquired during the SK89 expedition (onboard *ORV Sagar Kanya*, during January 1994; Kamesh Raju et al., 2004).

We estimated the age of oceanic crust underlying the Andaman Backarc Basin by employing forward modelling of magnetic profiles and by correlating them with the geomagnetic polarity reversal

timescale (Table 1) of Cande and Kent (1995). The magnetic anomaly picks that represent the younger and older boundaries of all the major normal polarity blocks are delineated by comparing the observed magnetic anomalies with the synthetic magnetic anomalies computed based on Talwani and Heirtzler (1964) method, using magnetized crustal block models. Having obtained the magnetic anomaly picks representing the locations and age of the magnetized block boundaries, we estimated the finite rotation parameters for selected timings, using the GPlates software (Boyden et al., 2011; Müller et al., 2018), to develop plate tectonic reconstruction maps to describe the evolution of the Andaman Backarc Basin.

4. Seafloor morphology of the Andaman Backarc Basin and the adjacent regions

The updated bathymetry map (Figure 3) of the Andaman Backarc Basin and the adjoining regions clearly depicts the presence of rift-valleys associated with segmented spreading centres in the axial part of the Andaman Backarc Basin. The map suggests the presence of four spreading segments, A, B, C, and D. The segments A, B, and C are located in the deep ocean basin between the Alcock and Sewell rises, while the segment D is located northeast of the Alcock Rise. A detailed account on the geomorphology of the segments A, B, and C was provided by Kamesh Raju et al. (2004). According to them, the rugged nature of bathymetry associated with the segments A and B might be due to the presence of volcanic constructs formed as a result of arc volcanism and the distinctly smooth nature of bathymetry over the segment C might represent a spreading centre filled with sediments derived from the Irrawaddy River. They further identified various fault systems that define the boundaries of various ridges and grabens as well as near-symmetrically emplaced seamounts on the conjugate sides of the spreading axis of segment A.

The high-resolution bathymetry maps (Figures 4a, b) of the eastern sector of the Andaman Backarc Basin, generated using a new set of multibeam bathymetry data, show that the segment D is characterized by nearly smooth seafloor topography, resulting from the sediment flow from the Irrawaddy River. This map clearly depicts the presence of three submarine channels, one of which (SC-1) is nearly straight while others (SC-2 and SC-3) are meandering in nature. These channels appear to terminate in the rift valley and are not traceable further south in the seafloor, probably due to the presence of thick sediments overlying them. The bathymetry map suggests that the segment is associated with a prominent, nearly E-W trending rift valley, represented by the isobaths ranging from 2850 to 2650 m. The bathymetry map presented as contours (in 25 m. interval) overlying the colour-coded image (Figure 4b) shows that the axis of the rift valley, defined by the deepest isobaths, differs from west to east. The rift valley is deepest (2850 m) near to its western part and it gently shallows towards east till it reaches to a seafloor depth of 2650 m at the easternmost region, where the axis of the rift valley joins with the Sagaing Fault. The width of the rift valley along the selected locations and

the variations in the depth to the seafloor along the rift valley axis are also depicted by the representation of the bathymetry extracted from the grid, plotted as track-along wiggles (Figure 5a, b).

Although the locations of the Alcock and Sewell rises were defined, various researchers (Rodolfo, 1969; Kamesh Raju et al., 2004; Curray, 2005; Morley and Alvey, 2015; Tripathi et al., 2019) used different boundaries to represent the shape and extent of these anomalous features, probably due to the unavailability of the adequate data. Delineation of the southern boundary of the Alcock Rise and the northern boundary of the Sewell Rise is important as this information can serve as a crucial constraint in defining the break-up of conjoint Alcock-Sewell Rise Complex and initiation of seafloor spreading in the Andaman Backarc Basin. We delineated the extent of the Alcock and Sewell rises (Figure 3) by considering the maximum slope defined by the bathymetry contours and colour-coded images derived from the multibeam bathymetry data. In the region where multibeam bathymetry data is not available, we used latest available GEBCO global bathymetry grid (GEBCO Compilation Group, 2020) to define the extent of the Alcock and Sewell rises. The updated bathymetry map (Figure 3) depicts the characteristics of the seafloor corresponding to the Andaman Transform Fault (ATF), which is an ~180 km long feature trending in nearly N-S direction. The nearly straight eastern boundary of the Alcock Rise appears to have shaped by the geometry of the Andaman Transform Fault, which represent the offset connecting the eastern side of the segment C with the western side of the segment D.

5. Magnetic anomaly signatures of the Andaman Backarc Basin

As explained earlier, the Andaman Backarc Basin consists of four spreading segments, A, B, C and D. A detailed account of the magnetic signatures in the segments A, B, and C was provided by Kamesh Raju et al. (2004). According to them, the segment A is associated with high-amplitude (~600 nT) magnetic anomalies; the segment B is associated with moderate-amplitude (~120-300 nT) magnetic anomalies; and the segment C is associated with low amplitude (~100 nT) and long wavelength (~100 km) magnetic anomalies. The source to the high amplitude magnetic anomalies was attributed to the volcanism, while the moderate-amplitude anomalies are considered to have formed by seafloor spreading. The cause for absence of significant magnetic anomalies over segment C was considered to be due to the low magnetization of the oceanic crust buried under the sediments. Recently, based on the analysis of multichannel seismic reflection data across the segment C of the Andaman Backarc Basin, Jourdain et al. (2016) suggested that the basaltic layer 2A of the oceanic crust, a primary source to the seafloor spreading magnetic anomalies, is replaced by a sill-sediment-metasedimentary layer, resulting in the absence of the magnetic anomalies. Subsequently, Kamesh Raju et al. (2020) evaluated this inference and supported this explanation for the creation of

nonmagnetic oceanic crust. If the above explanation is valid, then the segment D, which represents the fourth segment of the Andaman Backarc Basin spreading centre, should also be devoid of magnetic anomalies since this region is expected to have thicker sedimentation, due to its proximity to the Irrawaddy River in the north. To examine this concept, we acquired magnetic data across selected profiles over the segment D (Figure 6) and observed that segment D region is indeed devoid of significant magnetic anomalies and the anomaly signature is similar to that observed over segment C. The above observation corroborates the explanation provided by Jourdain et al. (2016) for absence of magnetic anomalies over sedimented spreading centres.

6. Revised plate tectonic evolution of the Andaman Backarc Basin

6.1 Revisit to the identification of magnetic anomalies

We present an updated magnetic anomaly map (Figure 7) of the segment B, using the magnetic profiles published by Kamesh Raju et al. (2004), integrated with the newly acquired magnetic profiles. We attempted to correlate the magnetic anomalies with the widely used polarity reversal timescale of Cande and Kent (1995), using the forward modelling of the magnetic anomalies by Talwani and Heirtzler (1964) method, to identify seafloor spreading magnetic anomalies and to infer the estimated age of the oceanic crust in the Andaman Backarc Basin. Synthetic anomalies were computed for juxtaposed normal and reversely magnetized oceanic crust striking 63° , assuming 2 km thickness and 1.25 A/m magnetization, and the block widths were considered assuming variable spreading rates (full spreading rates of 24 to 35 mm/yr) and the respective time intervals for the normal and reverse polarity interval defined by the timescale. These synthetic anomalies generated were compared with two representative observed profiles that span through the entire extent of the Andaman Backarc Basin (Figure 8) and the assumed spreading rates are refined until getting a reasonable good fit between the observed and computed magnetic anomalies.

Our model (Figure 9) suggests that the magnetic anomalies over the segment B of the Andaman Backarc Basin can be explained in terms of conjugate magnetic anomaly sequence C3An.1ny – 1n (5.894 – 0.0 Ma), formed with variable spreading rates (Table 2). During chrons C3An.1ny (5.894 Ma) to C3n.1ny (4.180 Ma), the seafloor was spreading with a full spreading rate of 24 mm/yr, resulting in symmetric seafloor spreading, accreting equal width of oceanic crust on both the flanks of the Andaman Backarc Basin. However, during the younger period, from chrons C3n.1ny (4.180 Ma) to C1no (0.780 Ma), we infer asymmetric spreading with a full spreading rate of 35 mm/yr. Again from chron Cn1o (0.780 Ma) onwards, symmetric seafloor spreading occurs with a full spreading rate of 24 mm/yr. Comparing the characteristic shape of the synthetic magnetic anomalies and the respective

locations of the block boundaries with the representative observed magnetic anomalies, we delineated the magnetic anomaly picks that represent the locations of younger and older boundaries of all the major magnetized crustal blocks of the oceanic crust (Figure 8). Further, these identifications are extended to the other profiles based on the correlation of the magnetic signatures and delineated the respective block boundaries (Figure 9). Based on this exercise, we created a high-resolution magnetic anomaly picks database for the Andaman Backarc Basin (see Supplementary Dataset DS-1). These picks were used to delineate the magnetic isochrons by connecting the magnetic anomaly picks representing the same age of the oceanic crust, and generated the revised high-resolution magnetic isochron chart of the Andaman Backarc Basin (Figure 10).

6.2 Breakup of Alcock-Sewell Rise Complex and formation of the Andaman Backarc Basin

The high-resolution magnetic isochron chart of the Andaman Backarc Basin shows that the oldest magnetic lineation present in this backarc basin corresponds to chron 3An.1ny (5.894 Ma), located immediately south of the Alcock Rise on the Burmese Plate. The conjugate of this oldest magnetic lineation on the Sunda Plate is located immediately north of the Sewell Rise. These observations suggest that the seafloor spreading in the Andaman Backarc Basin was initiated at around 5.9 Ma, by the breakup of the conjoint Alcock-Sewell Rise Complex.

To understand the pre-drift juxtaposition scenario of the Alcock and Sewell rises and the stage-by-stage evolution of the Andaman Backarc Basin, we attempted to estimate the total rotation parameters that describe the relative motion between Burmese and Sunda plates at selected timings using the magnetic anomaly picks derived from the present study. Normally, in the areas containing large number of spreading segments offset by fracture zones, the estimation of total rotation parameters is carried out using the magnetic anomaly picks and fracture zone crossings based on the statistical method of Hellinger (1981), as carried out in the Arabian and Eastern Somali basins (Royer et al., 2002), Central Indian Ocean (Cande et al., 2010; Cande and Patriat, 2015; Yatheesh et al., 2019), Wharton Basin (Jacob et al., 2014), etc. Since the Andaman Backarc Basin consists of only one segment and is devoid of well-defined fracture zones, we are unable to use the statistical method for estimating total rotation parameters. Considering this limitation, we computed the rotation parameters by fitting the selected conjugate magnetic anomaly picks by visually assuming a spreading direction perpendicular to the strike of the spreading segments, using the GPlates software (Boyden et al., 2011). Using these derived rotation parameters (Table 3) describing the relative motion between the Alcock and Sewell rises, we generated plate tectonic reconstruction maps (Figure 11a-d) depicting the stage-by-stage evolution of the Andaman Backarc Basin at four selected timings, C3An.1ny (5.894 Ma), C3n.1ny (4.180 Ma), C1no (0.780 Ma) and the Present (0.000 Ma), representing the timings of changes

in the spreading rates. The plate tectonic reconstruction model suggests that the Alcock and Sewell rises were juxtaposed to form a single unit and breakup of this conjoint Alcock-Sewell Rise Complex since C3An.1ny (5.894 Ma) resulted in the initiation of formation of the Andaman Backarc Basin (Figure 11a). The evidence to the timing of initiation of this breakup and subsequent seafloor spreading forming the Andaman Backarc Basin comes from the oldest magnetic lineations identified in the conjugate flanks of the Andaman Backarc Basin. Since then, the seafloor spreading continued at a full spreading rate of 24 mm/yr till chron C3n.1ny (Figure 11b), by accreting new oceanic crust on the Burmese Plate in the north and on the Sunda Plate in the south. Subsequently, seafloor spreading continued with an accelerated full spreading rate of 35 mm/yr and seafloor spreading with this spreading rate continued till chron Cn1o (Figure 11c). Further to this period, seafloor spreading continued with a decelerated full spreading rate of 24 mm/yr, resulting in the present day configuration of the Andaman Backarc Basin and the bordering Alcock and Sewell rises (Figure 11d).

The seafloor spreading history of the Andaman Backarc Basin derived from our magnetic investigation clearly shows that the Andaman Backarc Basin was formed by continual seafloor spreading from chrons C3An.1ny (5.894 Ma) to the present (0.000 Ma). The contrary interpretation of episodic seafloor spreading and reactivation for the formation of the Andaman Backarc Basin postulated by Morley (2015) and Morley and Alvey (2015) was based on the presence of 1 km thick sediment lying over the spreading centre that is supposed to have been constantly spreading at rates between 24-35 mm/yr. The recent hypothesis put forward by de Sagan and Olive (2021) on assessing the impact of sedimentation on fault spacing at the Andaman Backarc Basin spreading center provides a reasonable answer for the presence of thick sedimentation and the larger fault spacing as a function of plate separation accommodated by axial magmatic injection. In general, for the non-sedimented spreading centres, the widely spaced faults are associated with slower plate separation resulted by weak magma supply and the closely spaced faults are associated with faster plate separation resulted by robust magmatic emplacement. However, the observed large fault spacing at the Andaman Backarc Basin spreading centre was attributed to intense sedimentation along with robust magmatic emplacement, implying a continuous process of seafloor spreading (de Sagan and Olive, 2021). Further, if there was episodic seafloor spreading in the Andaman Backarc Basin, this should have been reflected in the India-Eurasia motion during post ~5.9 Ma. However, the recent study of DeMets et al. (2020) reported a regular and steady India-Eurasia plate motion since ~12.5 Ma.

7 Summary and conclusions

The updated bathymetry map of the Andaman Backarc Basin clearly shows that the region contains four spreading centre segments, A, B, C, and D, all of which are associated with well-defined

rift valleys. The newly mapped segment D, located east of the Alcock Rise, is characterized by nearly smooth seafloor topography, with a prominent, nearly E-W trending rift valley with a gentle dip from the west (where it is connected to the Andaman Transform Fault) to the east (where it is connected with the Sagaing Fault). We further delineated the extent and shape of the conjugate Alcock and Sewell rises and the ~180 km long Andaman Transform Fault that appears to have shaped the nearly straight eastern boundary of the Alcock Rise.

The absence of significant magnetic anomalies over segment C, which is buried under the sediments, was considered to be due to the low magnetization of the oceanic crust caused by the replacement of layer 2A by a sill-sediment-metasedimentary layer based on the seismic imaging. Our magnetic investigation over the segment D of the spreading centre, which is buried under the sediments, is also devoid of significant magnetic anomalies similar to the segment C. Therefore, we suggest that a similar process that explain the absence of magnetic anomalies over segment C (Jourdain et al., 2016; Kamesh Raju et al., 2020) is also possible over segment D. Although these inferences have come from the comparison of magnetic anomaly signatures with the seismic images, it is important to ground truth this inference of sub-horizontal sills injected within the sedimentary strata by deep ocean drilling in the Andaman Backarc Basin as proposed recently (Yatheesh et al., 2017; McKay et al., 2018).

We revisited the magnetic anomaly identifications in the Andaman Backarc Basin based on forward modelling of magnetic anomalies using a new set of data complemented by those used by Kamesh Raju et al. (2004). Our model suggests that the magnetic anomalies over the segment B of the Andaman Backarc Basin can reasonably be explained in terms of conjugate magnetic anomaly sequence C3An.1ny – 1n (5.894 – 0.0 Ma), formed with variable spreading rates. Seafloor spreading was symmetric with full spreading rate of 24 mm/yr during chrons C3An.1ny (5.894 Ma) to C3n.1ny (4.180 Ma); asymmetric with a full spreading rate of 35 mm/yr during chrons C3n1.ny (4.180 Ma) to C1no (0.780 Ma); and again symmetric with a full spreading rate of 24 mm/yr from chron Cn1o (0.780 Ma) till the present. We generated a magnetic anomaly picks database of the Andaman Backarc Basin that represent estimated age of the underlying oceanic crust, and generated the revised high-resolution magnetic isochron chart of the Andaman Backarc Basin. With this exercise, we revise the age of opening of the Andaman Backarc Basin from 4.0 Ma as suggested by Kamesh Raju et al. (2004) to ~5.9 Ma. Our analysis further establishes the continual seafloor spreading with variable spreading rates (full spreading rates of 24 to 35 mm/yr) in the Andaman Backarc Basin from ~5.9 Ma till the present, in contrary with the concept of episodic seafloor spreading and reactivation postulated by Morley (2015) and Morley and Alvey (2015).

The plate tectonic reconstruction maps generated using the rotation parameters estimated based on the magnetic anomaly picks suggest that the Andaman Backarc Basin was formed by the breakup of the conjoint Alcock-Sewell Rise Complex, starting from ~5.9 Ma. Although the age of opening of the Andaman Backarc Basin is well understood, the nature of crust underlying the Alcock and Sewell rises are yet to be established. A detailed understanding on genesis of these anomalous features are important to understand the overall plate kinematics associated with the formation and evolution of the Andaman Sea. Such information can be achieved by carrying out detailed seismic reflection and refraction experiments over these features and the adjoining areas in the Andaman Sea. Having obtained the velocity-depth structure of the Alcock and Sewell rises, the ground truth information can be obtained by deep ocean drilling over these features as proposed recently (Yatheesh et al., 2017; McKay et al., 2018).

Acknowledgment

The authors are grateful to Prof. Sunil Kumar Singh, Director, CSIR-NIO, for permission to publish this paper. KAK thanks Dr. M. Ravichandran, Director, NCPOR for support and encouragement. We are grateful to Mr. Korgaokar Mahesh and Mr. Rebello Sheldon from Research Vessel Management Group of CSIR-NIO for their excellent technical support throughout the expedition SSD-046 onboard *RV Sindhu Sadhana*. The support extended by Dr. Jensen Jacob, CSIR-NIO, in data acquisition is gratefully acknowledged. We also thank the Captain and crew members of SSD-046 expedition for their support extended in acquiring high-quality data. KKA thanks Department of Science and Technology, India, for providing the Inspire Fellowship (DST/INSPIRE-Fellowship/2015/IF150281). We are thankful to Prof. Chris Morley and an anonymous reviewer for their careful review of the manuscript and valuable comments. We are also grateful to Prof. Zheng-Xiang Li for editorial handling of the manuscript. This work forms a part of the TeAM-RiSe project, supported by Council of Scientific and Industrial Research, New Delhi. We used Mirone software (Luis, 2007) to handle the grid data and Generic Mapping Tools (Wessel et al., 2019) to plot all the figures presented in this paper. This is NIO contribution xxxx.

Figure captions

- Figure 1: Maps of the Andaman-Nicobar-Sumatra Subduction Zone and the adjacent regions defined by (a) GEBCO gridded bathymetry data (GEBCO Compilation Group, 2020) and (b) satellite-derived free-air gravity anomalies (Sandwell et al., 2014). ABB: Andaman Backarc Basin; MLP: Malay Peninsula; ALR: Alcock Rise; SWR: Sewell Rise; BI: Barren Island; NI: Narcondam Island
- Figure 2: Generalized tectonic map of the Andaman-Nicobar-Sumatra Subduction Zone and the adjacent regions. The dashed blue lines represent major faults (Kamesh Raju et al., 2004; Kamesh Raju et al., 2007; Tsutsumi and Sato, 2009; Cochran, 2010; Singh et al., 2013). The solid red triangles represent locations of the subaerial volcanoes (Sheth et al., 2009; Bandopadhyay, 2017), while the open red triangles represent locations of the submarine volcanoes together forming a volcanic arc (Kamesh Raju et al., 2004; Ghosal et al., 2012; Kamesh Raju et al., 2012; Tripathi et al., 2017; Aswini et al., 2020; Kamesh Raju et al., 2020). The thick continuous and dashed red lines represent the ridge axis and the associated transform faults, respectively (Kamesh Raju et al., 2004; This study). Black stars represent locations of the major earthquake events of 2004 and 2005. Blue coloured bold letters represent plate identifications. The extent of the Mergui Ridge and Sunda-Java Trench has been refined by taking into consideration the satellite-derived free-air gravity anomalies (Sandwell et al., 2014) and GEBCO gridded bathymetry data (GEBCO Compilation Group, 2020). The extent of Alcock Rise and Sewell Rise were refined based on the multibeam bathymetry data used in the present study, integrated with GEBCO gridded bathymetry data in the gap areas. EMF: Eastern Margin Fault; DLF: Diligent Fault; ANF: Andaman-Nicobar Fault; WAF: West Andaman Fault; ACF: Aceh Fault; SLF: Seulimeum Fault; GSF: Great Sumatra Fault; MNF: Mentawai Fault; ATF: Andaman Transform Fault; SGF: Sagaing Fault; IB: Invisible Bank; IND-Indian Plate; BUR: Burmese Plate; SUN: Sunda Plate. Other details are as in Figure 1.
- Figure 3: The updated bathymetry map of the Andaman Backarc Basin highlighting the regions of seafloor mapped by the shipborne multibeam bathymetry data along with the GEBCO gridded bathymetry data (GEBCO Compilation Group, 2020) in the background. Other details are as in Figure 2.
- Figure 4: High-resolution multibeam bathymetry map of the spreading segment D region of the Andaman Backarc Basin as depicted by (a) colour-coded multibeam bathymetry image and (b) colour-coded bathymetry contours in 25 m interval with bathymetric image in the background. The bathymetry contours with seafloor depth values less than 2650 m are given in grey colour. Other details are as in Figure 2.
- Figure 5: Bathymetry signature of the rift valley over the spreading segment D of the Andaman Backarc Basin as depicted (a) across the rift axis and (b) along the rift axis. These bathymetry signatures (shown as blue lines) were extracted from the bathymetry grid along the respective transects (shown as black lines). The thick continuous and dashed red lines represent the ridge axis and the associated transform faults, respectively.
- Figure 6: Magnetic anomalies across the spreading segment D in the Andaman Backarc Basin, plotted perpendicular to ship's tracks, along with the colour-coded bathymetric image in the background. Other details are as in Figures 2 and 4.

- Figure 7: Updated magnetic anomaly map over the spreading segment B in the Andaman Backarc Basin. The magnetic anomalies shown in back colour were obtained from Kamesh Raju et al. (2004), while those shown in blue colour represent new set of data acquired during the SSD-046 expedition. The labels shown as numbers within the circles represent profile identifications used in Figures 8 and 9. Other details are as in Figure 2.
- Figure 8: Observed and synthetic magnetic anomalies along selected profiles across the spreading segment B in the Andaman Backarc Basin. The major magnetized block boundaries are delineated over the profiles SSD46-03 and SK89r3+SSD46-04, by considering the magnetic signature in the synthetic magnetic profile and its correspondence in the magnetized block model. The numbers within the circles shown in purple fonts represent the profile identifications as shown in Figure 7.
- Figure 9: Approximate major boundaries of the normally and reversely magnetized blocks of the oceanic crust, representing major chrons of the geomagnetic polarity reversal timescale of Cande and Kent (1995) in the Andaman Backarc Basin. The profiles are stacked with respect to the location of the spreading axis. The numbers within the circles shown in purple fonts represent the profile identifications as shown in Figure 7. Other details are as in Figure 8.
- Figure 10: Maps showing (a) inferred boundaries of magnetized oceanic crustal blocks representing magnetic anomaly picks shown in Figure 9; and (b) revised high-resolution magnetic isochrons in the Andaman Backarc Basin. Other details are as in Figure 2.
- Figure 11: Simplified plate tectonic reconstruction maps depicting the stage-by-stage evolution of the Andaman Backarc Basin due to the relative motion of the Alcock Rise (Burmese Plate) and the Sewell Rise (Sunda Plate) in fixed Burmese Plate reference frame; (a) at chron C3An.1ny; (b) at chron C3n.1ny; (c) at chron Cn1o; (d) Present. ALR: Alcock Rise; SWR: Sewell Rise. Other details are as in Figure 10.

Table captions

- Table 1: Ages of the magnetic anomalies (chrons) after the magnetic polarity reversal timescale of Cande and Kent (1995). The young (y) and old (o) edges of magnetic anomalies refer to the end and beginning, respectively, of normal (n) polarity intervals.
- Table 2: Spreading rates derived based on the magnetic anomaly identifications for the northern and southern flanks of the Andaman Backarc Basin, depicting the asymmetric seafloor spreading during chrons C1no (0.780 Ma) to C3n.1ny (4.180 Ma) at Burmese-Sunda plate boundary. Fourth and Sixth columns in the table represent half spreading rates (HSR), while the last column in the table represents the full spreading rates (FSR).
- Table 3: Finite rotation parameters describing relative motions between Alcock Rise (Burmese Plate) and Sewell Rise (Sunda Plate) through Andaman Backarc Basin, in fixed Burmese plate reference frame. Angle is positive when the motion of the moving plate is counter clockwise with respect to the fixed plate when viewed from outside the earth. Ages are after Cande and Kent (1995).

References

- Aswini, K.K., Dewangan, P., Kamesh Raju, K.A., Yatheesh, V., Singha, P., Arya, L., Ramakrushana Reddy, T., 2020. Sub-surface magma movement inferred from low-frequency seismic events in the off-Nicobar region, Andaman Sea. *Sci. Rep.* 10, 21219.
- Bandopadhyay, P.C., 2017. Inner-arc volcanism: Barren and Narcondam islands, in: Bandopadhyay, P.C., Carter, A. (Eds.), *The Andaman–Nicobar Accretionary Ridge: Geology, Tectonics and Hazards*. *Geol. Soc. Lond. Mem.* 47, pp. 167–192.
- Boyden, J.A., Müller, R.D., Gurnis, M., Torsvik, T.H., Clark, J.A., Turner, M., Ivey-Law, H., Watson, R.J., Cannon, J.J., 2011. Next-generation plate-tectonic reconstructions using GPlates, in: Keller, G.R., Baru, C. (Eds.), *Geoinformatics: Cyberinfrastructure for the Solid Earth Sciences*. Cambridge University Press, pp. 95–114.
- Cande, S.C., Kent, D.V., 1995. Revised calibration of the geomagnetic polarity time scale for the Late Cretaceous and Cenozoic. *J. Geophys. Res.* 100, 6093–6095.
- Cande, S.C., Patriat, P., 2015. The anticorrelated velocities of Africa and India in the Late Cretaceous and early Cenozoic. *Geophys. J. Int.* 200, 227–243.
- Cande, S.C., Patriat, P., Dymant, J., 2010. Motion between the Indian, Antarctic and African plates in the early Cenozoic. *Geophys. J. Int.* 183, 127–149.
- Cochran, J.R., 2010. Morphology and tectonics of the Andaman Forearc, northeastern Indian Ocean. *Geophys. J. Int.* 182, 631–651.
- Curray, J.R., 2005. Tectonics and history of the Andaman Sea region. *J. Asian Earth Sci.* 25, 187–232.
- Curray, J.R., Moore, D.G., Lawver, L.A., Emmel, F.J., Raitt, R.W., Henry, M., Kieckhefer, R., 1979. Tectonics of the Andaman Sea and Burma, in: Wartkins, J., Montadert, L., Dickerson, P.W. (Eds.), *Geological and Geophysical Investigations of Continental margins*. AAPG Memoir 29, pp. 189–198.
- DeMets, C., Merkouriev, S., Jade, S., 2020. High-resolution reconstructions and GPS estimates of India–Eurasia and India–Somalia plate motions: 20 Ma to the present. *Geophys. J. Int.* 220, 1149–1171.
- de Sagazan, C., Olive, J.-A., 2021. Assessing the impact of sedimentation on fault spacing at the Andaman Sea spreading center. *Geology* 49, 447–451.
- Diehl, T., Waldhauser, F., Cochran, J.R., Kamesh Raju, K.A., Seeber, L., Schaff, D., Engdahl, E.R., 2013. Back-arc extension in the Andaman Sea: Tectonic and magmatic processes imaged by high-precision teleseismic double-difference earthquake relocation. *J. Geophys. Res. Solid Earth* 118, 2206–2224.
- GEBCO Compilation Group, 2020. GEBCO 2020 Grid, doi:10.5285/a29c5465-b138-234d-e053-6c86abc040b9.
- Ghosal, D., Singh, S.C., Chauhan, A.P.S., Hananto, N.D., 2012. New insights on the offshore extension of the Great Sumatran fault, NW Sumatra, from marine geophysical studies. *Geochem. Geophys. Geosyst.* 13, Q0AF06, doi:10.1029/2012GC004122.

- Hellinger, S.J., 1981. The uncertainties of finite rotations in plate tectonics. *J. Geophys. Res.* 86, 9312-9318.
- Jacob, J., Dymant, J., Yatheesh, V., 2014. Revisiting the structure, age and evolution of the Wharton basin to better understand subduction under Indonesia. *J. Geophys. Res.* 119, 169–190.
- Jha, P., Ros, D., DeglialessandrinI, A., 2008. Evolution and hydrocarbon occurrences of rift basins at the western margin of Sunda platform and relations with East Andaman Basin, GEO India Convention & Exhibition, New Delhi, India, pp. 16-19.
- Jourdain, A., Singh, S.C., Escartin, J., Klinger, Y., Kamesh Raju, K.A., McArdle, J., 2016. Crustal accretion at a sedimented spreading center in the Andaman Sea. *Geology* 44, 351-354.
- Kamesh Raju, K.A., Aswini, K.K., Yatheesh, V., 2020. Tectonics of the Andaman Backarc Basin - Present Understanding and Some Outstanding Questions, in: Ray, J.S., Radhakrishna, M. (Eds.), *The Andaman Islands and Adjoining Offshore: Geology, Tectonics and Palaeoclimate*. Springer International Publishing, Cham, pp. 237-259.
- Kamesh Raju, K.A., Murty, G.P.S., Amarnath, D., Kumar, M.L.M., 2007. The west Andaman fault and its influence on the aftershock pattern of the recent megathrust earthquakes in the Andaman-Sumatra region. *Geophys. Res. Lett.* 34, L03305, doi:10.1029/2006GL028730.
- Kamesh Raju, K.A., Ramprasad, T., Rao, P.S., Ramalingeswara Rao, B., Varghese, J., 2004. New insights into the tectonic evolution of the Andaman basin, northeast Indian Ocean. *Earth Planet. Sci. Lett.* 221, 145-162.
- Kamesh Raju, K.A., Ray, D., Mudholkar, A., Murty, G.P.S., Gahalaut, V.K., Samudrala, K., Paropkari, A.L., Ramachandran, R., Surya Prakash, L., 2012. Tectonic and volcanic implications of a cratered seamount off Nicobar Island, Andaman Sea. *J. Asian Earth Sci.* 56, 42-53.
- Luis, J.F., 2007. Mirone: A multi-purpose tool for exploring grid data. *Comput. Geosci.* 33, 31-41.
- McKay, R., Exon, N., Müller, D., Gohl, K., Gurnis, M., Shevenell, A., Henrys, S., Inagaki, F., Pandey, D.K., Whiteside, J., van de Flierdt, T., Naish, T., Heuer, V., Morono, Y., Coffin, M., Godard, M., Wallace, L., Kodaira, S., Bijl, P., Collot, J., Dickens, G., Dugan, B., Dunlea, A.G., Hackney, R., Ikehara, M., Jutzeler, M., McNeill, L., Naik, S., Noble, T., Opdyke, B., Pecher, I., Stott, L., Uenzelmann-Neben, G., Yatheesh, V., Wortmann, U.G., 2018. Developing community-based scientific priorities and new drilling proposals in the southern Indian and southwestern Pacific oceans. *Sci. Drill.* 24, 61-70.
- Morley, C.K., 2015. Cenozoic structural evolution of the Andaman Sea: evolution from an extensional to a sheared margin, in: Morley, C.K., Nemčok, M., Rybár, S., Sinha, S.T., Hermeston, S.A., Ledvényiová, L. (Eds.), *Transform Margins: Development, Controls and Petroleum Systems*. Geol. Soc. Lond. Spec. Publ. 431, pp. 39-61.
- Morley, C.K., 2017. Cenozoic rifting, passive margin development and strike-slip faulting in the Andaman Sea: a discussion of established v. new tectonic models. Geological Society, London, Mem. 47, 27-50.
- Morley, C.K., Alvey, A., 2015. Is spreading prolonged, episodic or incipient in the Andaman Sea? Evidence from deepwater sedimentation. *J. Asian Earth Sci.* 98, 446-456.

- Morley, C.K., Searle, M., 2017. Regional tectonics, structure and evolution of the Andaman–Nicobar Islands from ophiolite formation and obduction to collision and back-arc spreading. Geological Society, London, Mem. 47, 51-74.
- Mukti, M.M., 2018. Structural complexity in the boundary of forearc basin – accretionary wedge in the northwesternmost Sunda active margin. Bull. Mar. Geol. 33, 1-14.
- Müller, R.D., Cannon, J., Qin, X., Watson, R.J., Gurnis, M., Williams, S., Pfaffelmoser, T., Seton, M., Russell, S.H.J., Zahirovic, S., 2018. GPlates: Building a Virtual Earth Through Deep Time. *Geochem. Geophys. Geosyst.* 19, 2243-2261.
- Polachan, S., Racey, A., 1994. Stratigraphy of the Mergui Basin, Andaman Sea: Implications for petroleum exploration. *J. Petrol. Geol.* 17, 373-406.
- Rodolfo, K., 1969. Bathymetry and Marine Geology of the Andaman Basin, and Tectonic Implications for Southeast Asia. *Geol. Soc. Am. Bull.* 80, 1203-1230.
- Roy, S.K., Sharma, S.D., 1993. Evolution of Andaman Forearc Basin and its hydrocarbon potential, in: Biswas, S.K. (Ed.), *Proceeding of the Second Seminar on Petroliferous Basins of India*. Indian Petroleum Publishers., Dehra Dun, pp. 407-435.
- Royer, J.Y., Chaubey, A.K., Dymant, J., Bhattacharya, G.C., Srinivas, K., Yatheesh, V., Ramprasad, T., 2002. Paleogene plate tectonic evolution of the Arabian and Eastern Somali basins, in: Clift, P.D., Croon, D., Gaedicke, C., Craig, J. (Eds.), *The Tectonic and Climatic Evolution of the Arabian Sea Region*. *Geol. Soc. Lond. Spec. Publ.* 195, pp. 7-23.
- Sandwell, D.T., Müller, R.D., Smith, W.H.F., Garcia, E., Francis, R., 2014. New global marine gravity model from CryoSat-2 and Jason-1 reveals buried tectonic structure. *Science* 346, 65-67.
- Sheth, H.C., Ray, J.S., Bhutani, R., Kumar, A., Smitha, R.S., 2009. Volcanology and eruptive styles of Barren Island: an active mafic stratovolcano in the Andaman Sea, NE Indian Ocean. *Bull. Volcanol.* 71, 1021, doi: 10.1007/s00445-00009-00280-z.
- Singh, S.C., Moeremans, R., 2017. Anatomy of the Andaman–Nicobar subduction system from seismic reflection data, in: Bandopadhyay, P.C., Carter, A. (Eds.), *The Andaman–Nicobar Accretionary Ridge: Geology, Tectonics and Hazards*, *Geol. Soc. Lond. Mem.* 47, pp. 193-204.
- Singh, S.C., Moeremans, R., McArdle, J., Johansen, K., 2013. Seismic images of the sliver strike-slip fault and back thrust in the Andaman-Nicobar region. *J. Geophys. Res. Solid Earth* 118, 5208-5224.
- Srisuriyon, K., Morley, C.K., 2014. Pull-apart development at overlapping fault tips: Oblique rifting of a Cenozoic continental margin, northern Mergui Basin, Andaman Sea. *Geosphere* 10, 80-106.
- Talwani, M., Heirtzler, J.R., 1964. Computation of Magnetic anomalies caused by two dimensional structures of arbitrary shape, in: Parks, G.A. (Ed.), *Computers in the Mineral Industries*. Stanford University, pp. 464-480.
- Tripathi, S.K., Nagendran, G., Karthikeyan, M., Vasu, P., Tripathy, S.K., Varghese, S., Raghav, S., Resmi, S., 2017. Morphology of submarine volcanic seamounts from inner volcanic arc of Andaman Sea. *Indian J. Geosci.* 71, 451–470.

- Tripathi, S.K., Sathikumar, R., Kaustubhakumari, J.B., Guha, P.D., Meitei, S.I., 2019. Genesis and morphotectonic characterisation of crescent-shaped feature from Alcock Rise, Andaman Sea. *Bull. Mar. Geol.* 34, 89-104.
- Tsutsumi, H., Sato, T., 2009. Tectonic Geomorphology of the Southernmost Sagaing Fault and Surface Rupture Associated with the May 1930 Pegu (Bago) Earthquake, Myanmar. *Bull. Seismol. Soc. Am.* 99, 2155-2168.
- Wessel, P., Luis, J.F., Uieda, L., Scharroo, R., Wobbe, F., Smith, W.H.F., Tian, D., 2019. The Generic Mapping Tools Version 6. *Geochem. Geophys. Geosyst.* 20, 5556-5564.
- Yatheesh, V., Dymant, J., Bhattacharya, G.C., Royer, J.Y., Kamesh Raju, K.A., Ramprasad, T., Chaubey, A.K., Patriat, P., Srinivas, K., Choi, Y., 2019. Detailed structure and plate reconstructions of the Central Indian Ocean between 83.0 and 42.5 Ma (Chronos 34 and 20). *J. Geophys. Res. Solid Earth* 124, 4305-4322.
- Yatheesh, V., Pandey, D.K., Kamesh Raju, K.A., Nair, N., Pandey, A., Dewangan, P., Naik, S., Nath, B.N., Singh, S., Mudholkar, A.V., 2017. A proposal for deep ocean drilling in backarc and forearc of the Andaman Subduction Zone, Australasian IODP Regional Planning Workshop, University of Sydney, Australia, p. 52.

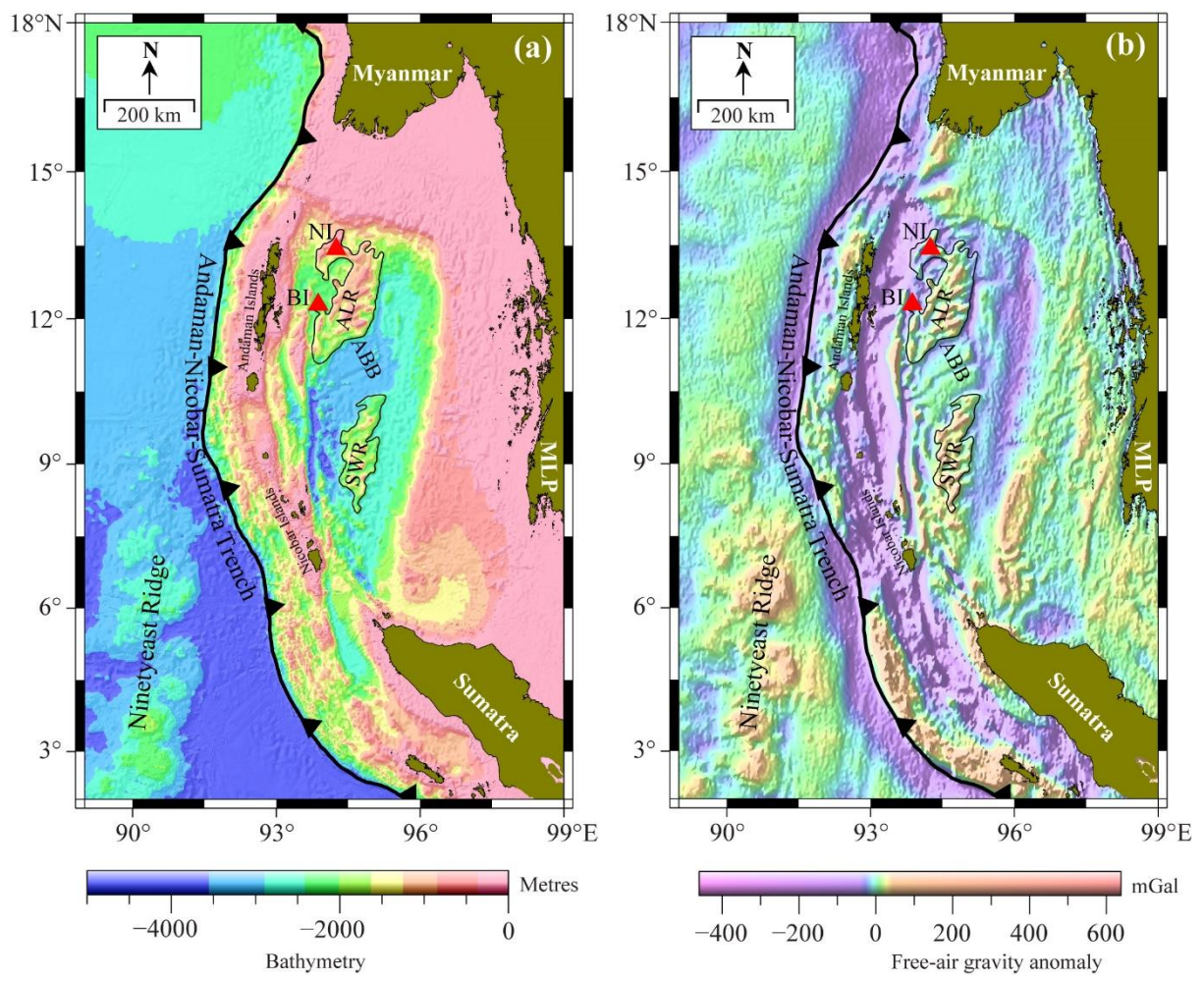


Figure 1

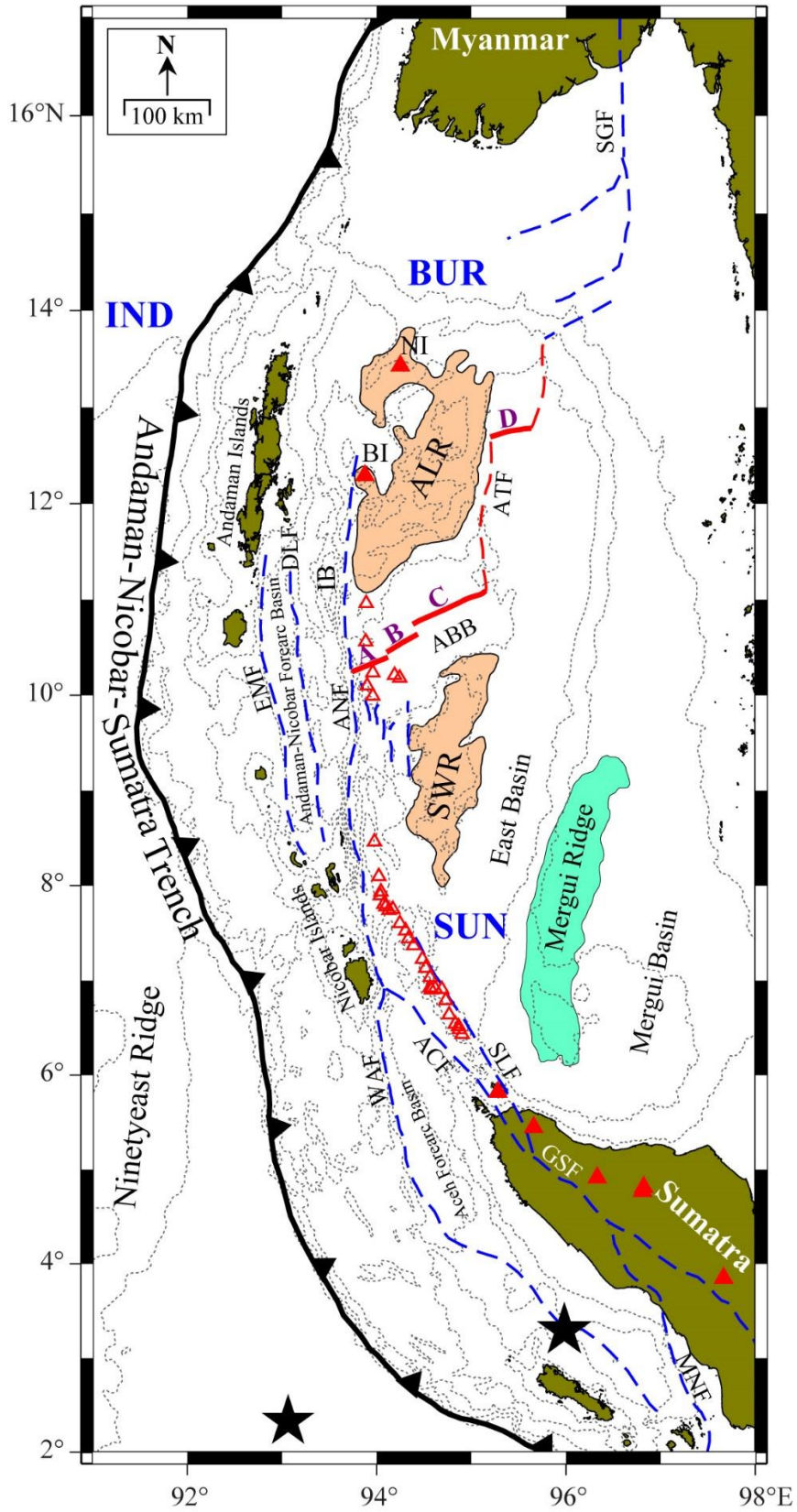


Figure 2

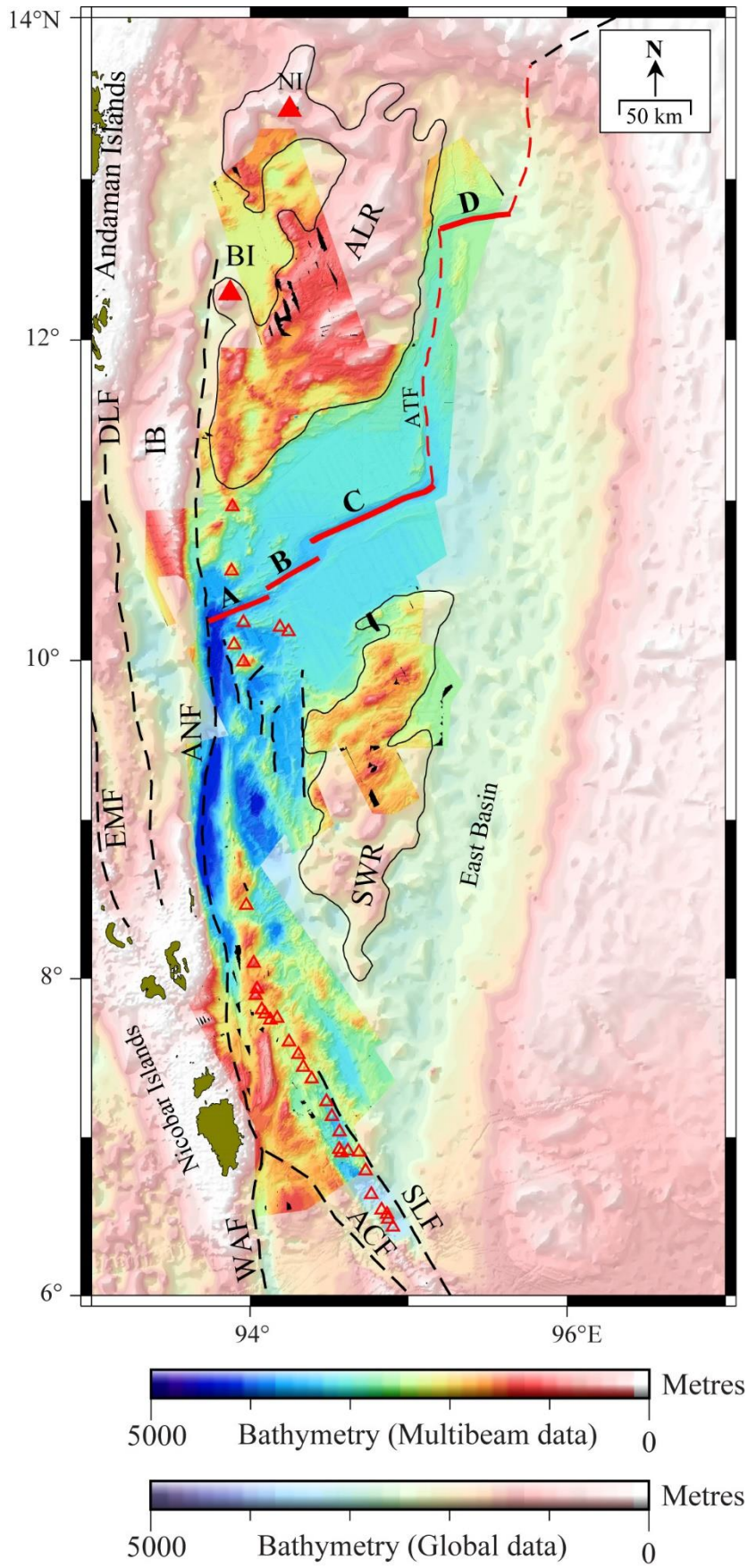


Figure 3

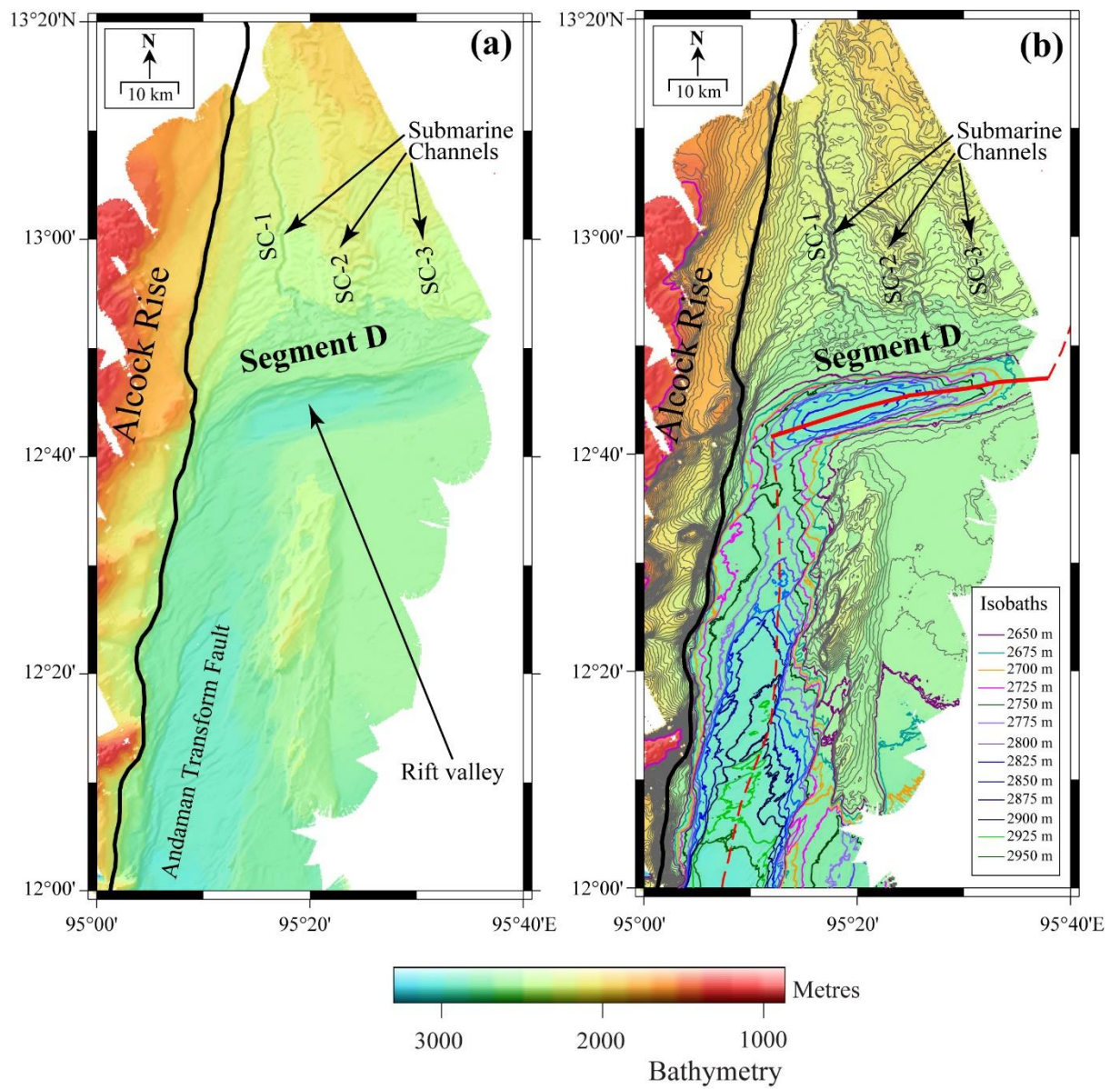


Figure 4

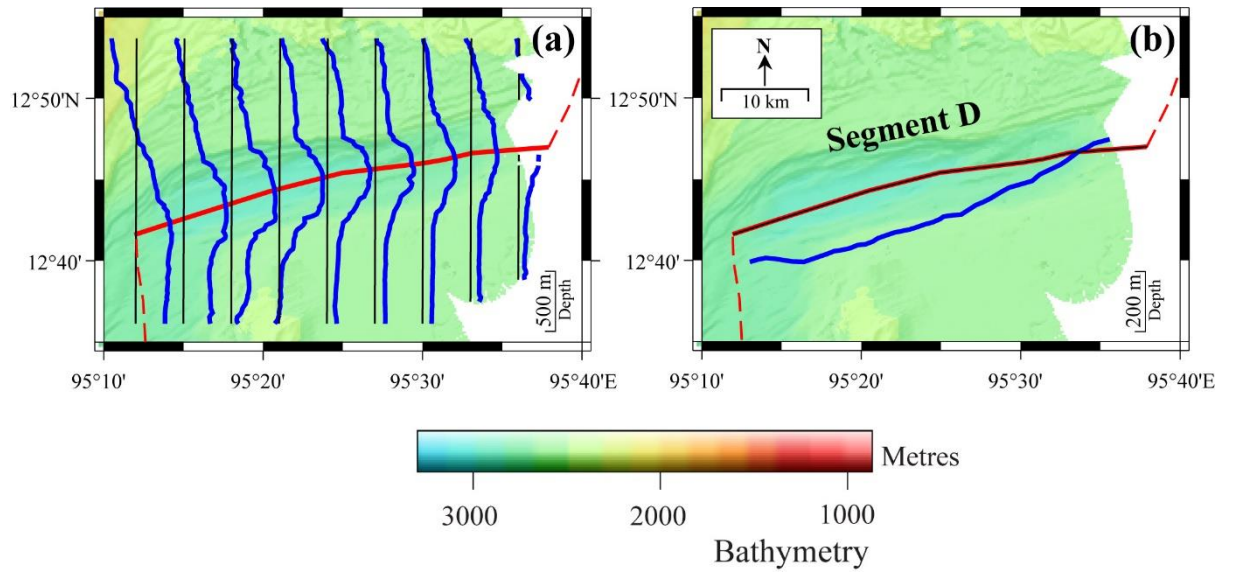


Figure 5

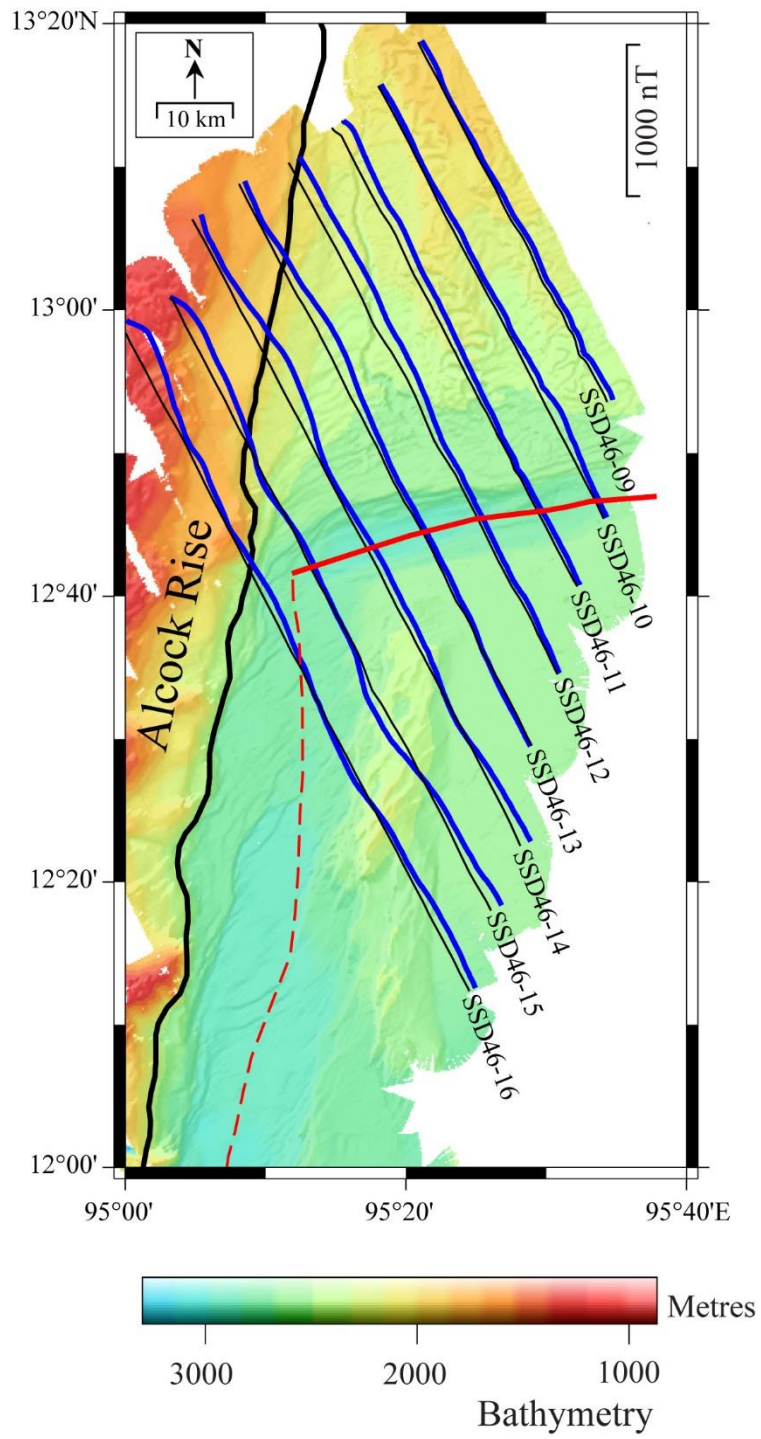


Figure 6

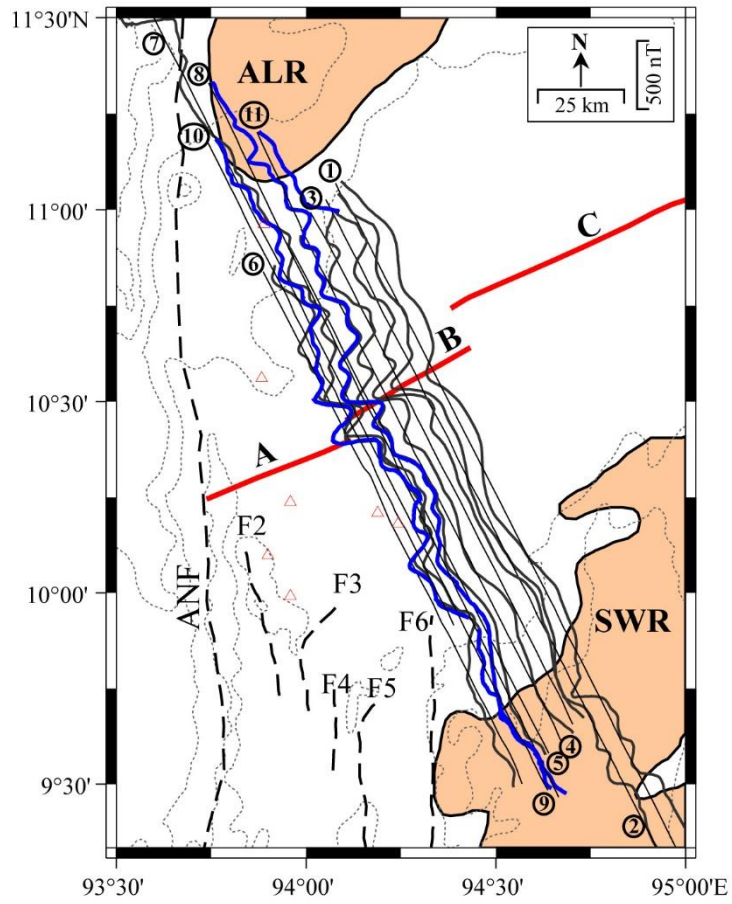


Figure 7

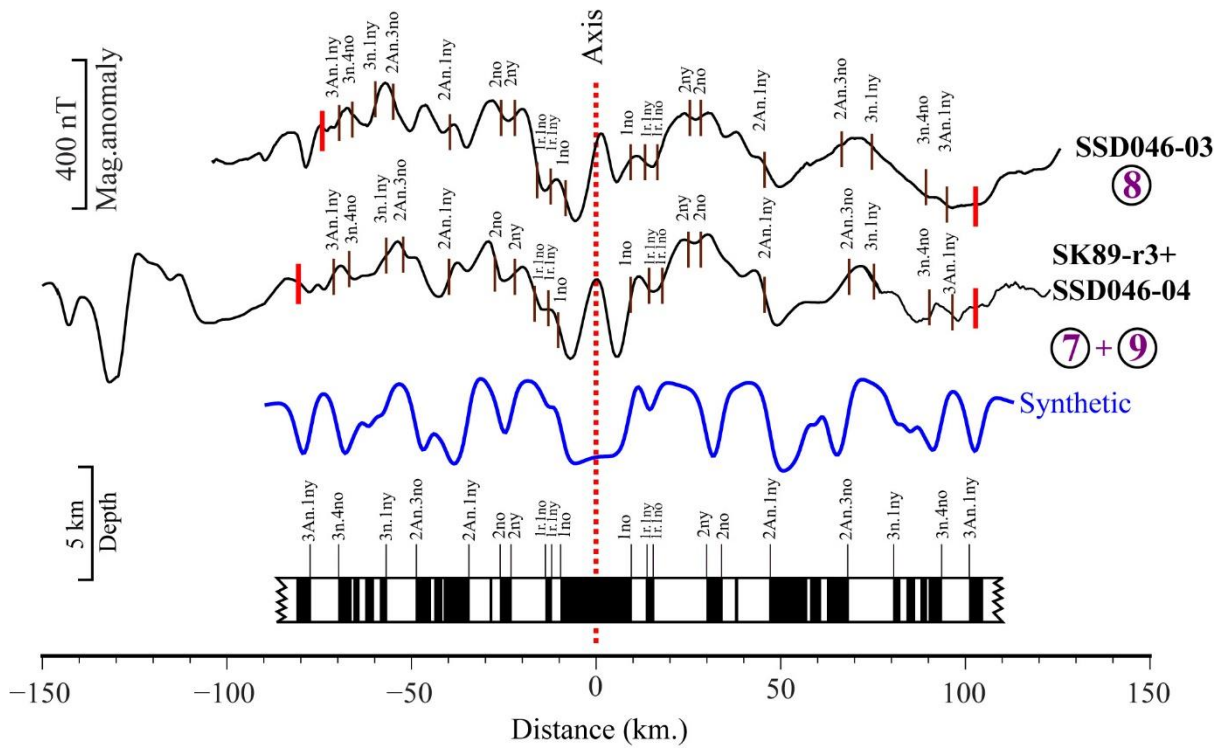


Figure 8

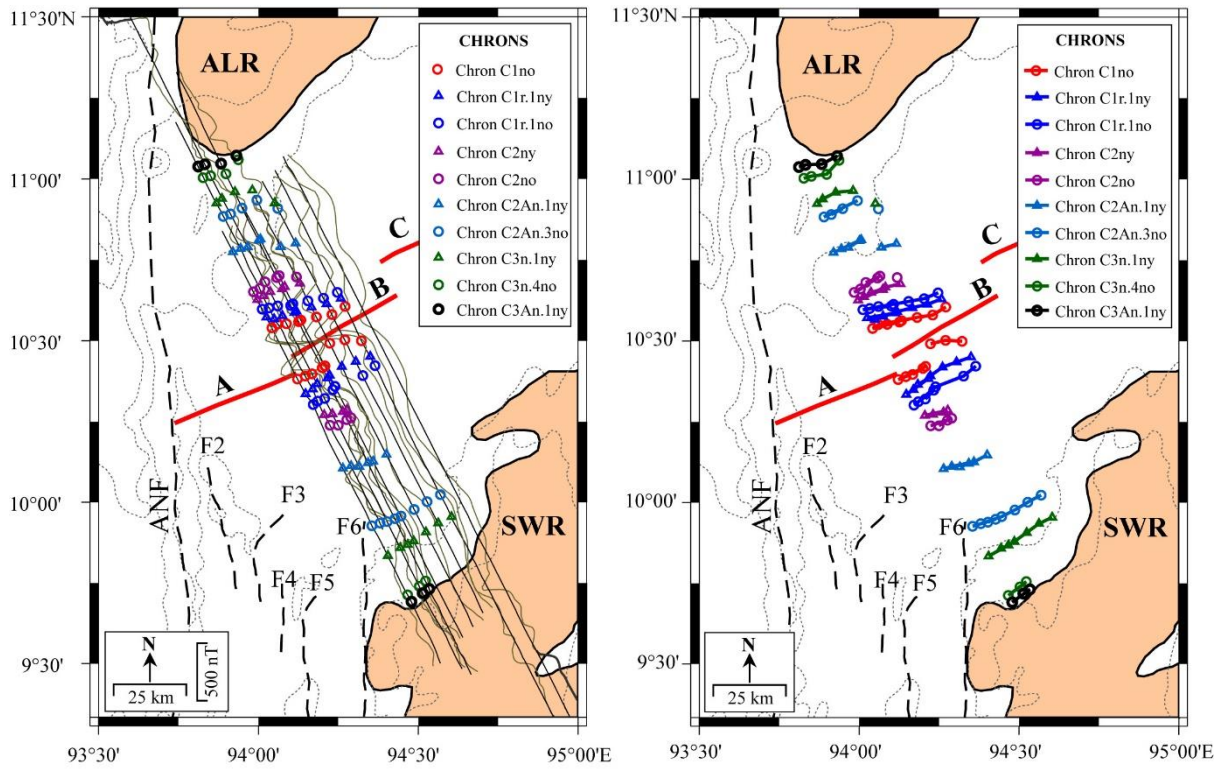


Figure 10

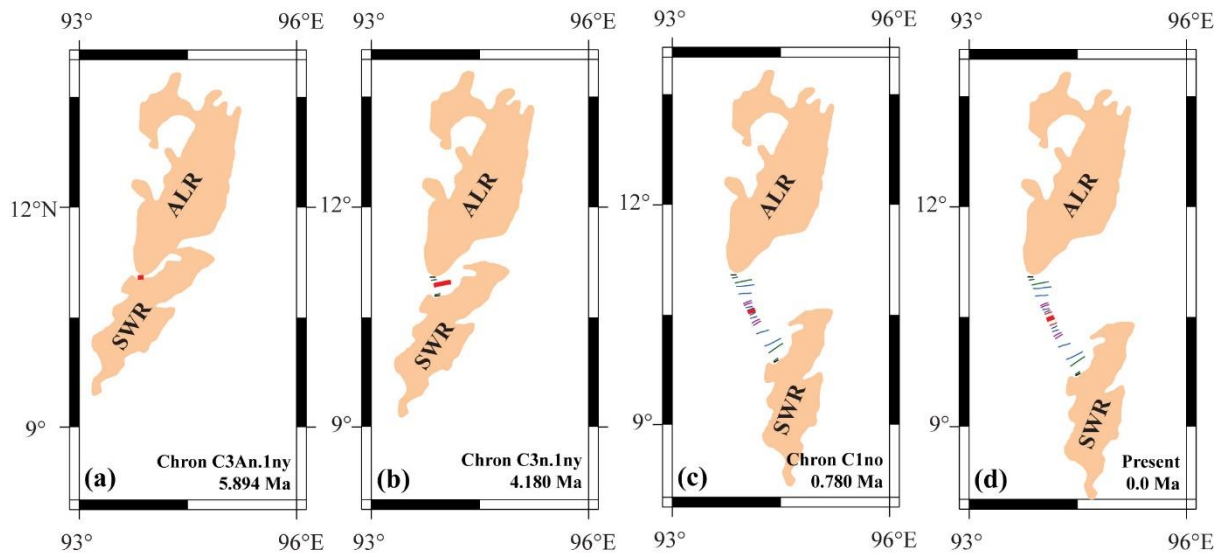


Figure 11

Chronos	Young edge (Ma)	Old edge (Ma)
C1n	0.000	0.780
C1r.1n	0.990	1.070
C2n	1.770	1.950
C2r.1n	2.140	2.150
C2An.1n	2.581	3.040
C2An.2n	3.110	3.220
C2An.3n	3.330	3.580
C3n.1n	4.180	4.290
C3n.2n	4.480	4.620
C3n.3n	4.800	4.890
C3n.4n	4.980	5.230
C3An.1n	5.894	6.137

Table 1

Chronos	Duration (m.y.)	Northern flank		Southern flank			Total
		Distance (km)	HSR (mm/yr)	Distance (km)	HSR (mm/yr)	Distance (km)	FSR (mm/yr)
C1ny - C1no	0.780	9.36	12	9.36	12	18.72	24
C1no - C1r.1ny	0.210	2.94	14	4.41	21	7.35	35
C1r.1ny - C1r.1no	0.080	1.12	14	1.68	21	2.80	35
C1r.1no - C2ny	0.700	9.80	14	14.70	21	24.50	35
C2ny - C2no	0.180	2.52	14	3.78	21	6.30	35
C2no - C2An.1ny	0.631	8.83	14	13.25	21	22.09	35
C2An.1ny - C2An.3no	0.999	13.99	14	20.98	21	34.97	35
C2An.3no - C3n.1ny	0.600	8.40	14	12.60	21	21.00	35
C3n.1ny - C3n.4no	1.050	12.60	12	12.60	12	25.20	24
C3n.4no - C3An.1ny	0.664	7.97	12	7.97	12	15.94	24

Table 2

Chron	Age (Ma)	Finite rotation parameters		
		Lat. (deg.)	Long. (deg.)	Angle (deg.)
C1ny	0.000	11.65	96.88	0.00
C1no	0.780	11.65	96.88	-3.25
C1r.1ny	0.990	11.65	96.88	-4.60
C1r.1no	1.070	11.65	96.88	-6.25
C2ny	1.770	11.65	96.88	-8.20
C2no	1.950	11.65	96.88	-9.40
C2An.1ny	2.581	11.65	96.88	-14.50
C2An.3no	3.580	11.65	96.88	-20.30
C3n.1ny	4.180	11.65	96.88	-23.30
C3n.1ny	5.200	11.65	96.88	-27.11
C3An.1ny	5.894	11.65	96.88	-28.25

Table 3